

- Henderson, L. E., Hewetson, J. F., Hopkins, R. F., Sowder, R. C., Neubauer, R. H., & Rabin, H. (1983) *J. Immunol.* 131, 810-815.
- Holley, R. W., Armour, R., & Baldwin, J. H. (1978) *Proc. Natl. Acad. Sci. U.S.A.* 75, 1864-1866.
- Holley, R. W., Armour, R., & Baldwin, J. H. (1980) *Proc. Natl. Acad. Sci. U.S.A.* 77, 5989-5992.
- Hunkapiller, M. W., & Hood, L. E. (1983) *Science (Washington, D.C.)* 219, 650-659.
- Kaighn, M. E., Narayan, K. S., Ohnuki, Y., Lechner, J. F., & Jones, L. W. (1979) *Invest. Urol.* 17, 16-23.
- Kaighn, M. E., Lechner, J. F., Babcock, M. S., Marnell, M., Ohnuki, Y., & Narayan, K. S. (1980) in *Models for Prostatic Cancer* (Murphy, G. P., Ed.) pp 85-109, Alan R. Liss, New York, NY.
- Laemmli, U. K. (1970) *Nature (London)* 227, 680-685.
- Marquardt, H., & Todaro, G. J. (1982) *J. Biol. Chem.* 257, 5220-5225.
- Merril, C. R., Goldman, D., Sedman, S. A., & Ebert, M. H. (1981) *Science (Washington, D.C.)* 211, 1437-1438.
- Seyedin, S. M., Thomas, T. C., Thompson, A. Y., Rosen, D. M., & Piez, K. A. (1985) *Proc. Natl. Acad. Sci. U.S.A.* 82, 2267-2271.
- Seyedin, S. M., Segarini, P. R., Rosen, D. M., Thompson, A. Y., Bentz, H., & Graycar, J. (1987) *J. Biol. Chem.* 262, 1946-1949.
- Sporn, M. B., & Todaro, G. J. (1980) *N. Engl. J. Med.* 303, 878-880.
- Sporn, M. B., & Roberts, A. B. (1985) *Nature (London)* 313, 745-747.
- Sporn, M. B., Roberts, A. B., Wakefield, L. M., & Assoian, R. K. (1986) *Science (Washington, D.C.)* 233, 532-534.
- Todaro, G. J., De Larco, J. E., Fryling, C., Johnson, P. A., & Sporn, M. B. (1981) *J. Supramol. Struct.* 15, 287-301.
- Tucker, R. F., Shipley, G. D., Moses, H. L., & Holley, R. W. (1984) *Science (Washington, D.C.)* 226, 705-707.

## Articles

### Structure of the High-Affinity Binding Site for Noncompetitive Blockers of the Acetylcholine Receptor: [<sup>3</sup>H]Chlorpromazine Labels Homologous Residues in the $\beta$ and $\delta$ Chains<sup>†</sup>

Jérôme Giraudat,<sup>†</sup> Michael Dennis,<sup>†</sup> Thierry Heidmann,<sup>†</sup> Pierre-Yves Haumont,<sup>§</sup> Florence Lederer,<sup>§</sup> and Jean-Pierre Changeux<sup>\*,†</sup>

Unité de Neurobiologie Moléculaire et Unité Associée au Centre National de la Recherche Scientifique UA 041149, Interactions Moléculaires et Cellulaires, Département des Biotechnologies, Institut Pasteur, 75724 Paris Cédex 15, France, and Unité 25 de l'Institut National de la Santé et de la Recherche Médicale et Laboratoire Associé au Centre National de la Recherche Scientifique LA 122, Hôpital Necker, 75730 Paris Cédex 15, France

Received July 22, 1986; Revised Manuscript Received October 10, 1986

**ABSTRACT:** The membrane-bound acetylcholine receptor from *Torpedo marmorata* was photolabeled by the noncompetitive channel blocker [<sup>3</sup>H]chlorpromazine under equilibrium conditions in the presence of the agonist carbamoylcholine. The amount of radioactivity incorporated into all subunits was reduced by addition of phencyclidine, a specific ligand for the high-affinity site for noncompetitive blockers. The labeled  $\beta$  chain was purified and digested with trypsin or CNBr, and the resulting fragments were fractionated by high-performance liquid chromatography. Sequence analysis resulted in the identification of Ser-254 and Leu-257 as residues labeled by [<sup>3</sup>H]chlorpromazine in a phencyclidine-sensitive manner. These residues are located in the hydrophobic and potentially transmembrane segment M II of the  $\beta$  chain, a region homologous to that containing the chlorpromazine-labeled Ser-262 in the  $\delta$  chain [Giraudat, J., Dennis, M., Heidmann, T., Chang, J. Y., & Changeux, J.-P. (1986) *Proc. Natl. Acad. Sci. U.S.A.* 83, 2719-2723]. These results show that homologous regions of different receptor subunits contribute to the unique high-affinity site for noncompetitive blockers, a finding consistent with the location of this site on the axis of symmetry of the receptor molecule.

**T**he nicotinic acetylcholine receptor (AChR)<sup>1</sup> from fish electric organ and vertebrate neuromuscular junction is a

heterologous pentamer ( $\alpha_2\beta\gamma\delta$ ) that both carries the acetylcholine binding sites at the level of the  $\alpha$  chains and contains the agonist-gated ion channel [reviews in Changeux et al. (1984), Anholt et al. (1985) and Stroud and Finer-Moore

<sup>†</sup> This work was supported by grants from the Muscular Dystrophy Association of America, the Collège de France, the Ministère de la Recherche et de l'Enseignement Supérieur, the Centre National de la Recherche Scientifique, and the Commissariat à l'Energie Atomique. M.D. is the recipient of a fellowship from the Fonds de la Recherche en Santé du Québec.

<sup>‡</sup> Institut Pasteur.

<sup>§</sup> Hôpital Necker.

<sup>1</sup> Abbreviations: AChR, acetylcholine receptor; NCB, noncompetitive blocker; CPZ, chlorpromazine; NaDodSO<sub>4</sub>, sodium dodecyl sulfate; PTH-amino acids, phenylthiohydantoin amino acids; HPLC, high-performance liquid chromatography; TPCK, N<sup>α</sup>-tosylphenylalanine chloromethyl ketone; AUFS, absorbance units full scale.

(1985)]. The complete primary structure of the AcChR subunits has been established by DNA cloning and sequencing in *Torpedo californica* ( $\alpha$ ,  $\beta$ ,  $\gamma$ , and  $\delta$ ) (Noda et al., 1983b; Claudio et al., 1983), *Torpedo marmorata* ( $\alpha$ ) (Devillers-Thiery et al., 1983), and various other species [review in Stroud and Finer-Moore (1985)].

The subunits have a high degree of sequence homology, and in particular all of them display two hydrophilic domains and four hydrophobic segments (M I–M IV). Several models of the transmembrane organization of the AcChR have been inferred from these primary structure data. They assume that at least some of the hydrophobic segments are transmembrane, possibly arranged in  $\alpha$ -helices, and that the subunits are symmetrically organized around the ion channel (Noda et al., 1983b; Claudio et al., 1983; Devillers-Thiery et al., 1983; Guy, 1984; Finer-Moore & Stroud, 1984; Ratnam et al., 1986). By hydrophobic labeling of the membrane-bound AcChR using photoactivable phospholipids, we previously demonstrated that, in agreement with such models, all AcChR subunits are exposed to the lipid bilayer (Giraudat et al., 1985). In the present study, we provide evidence for a symmetrical organization of the AcChR chains at the level of the high-affinity binding site for noncompetitive blockers (NCBs).

The NCBs comprise a heterogeneous group of compounds that block the permeability response to acetylcholine by interfering directly and/or indirectly with the functioning of the ion channel [reviewed in Neher and Steinbach (1978), Adams (1981), and Changeux et al. (1984)]. NCBs reversibly interact, under equilibrium conditions, with a few categories of sites present on the membrane-bound AcChR. The most prominent one is a high-affinity site that binds the frog toxin histrionicotoxin or the hallucinogen phencyclidine, is distinct from but allosterically coupled to the acetylcholine binding sites, and is present as a single copy per AcChR oligomer [reviewed in Heidmann et al. (1983)]. Covalent labeling of this high-affinity site has been selectively achieved by using a variety of NCBs under equilibrium conditions. Depending on the ligand and on the species of *Torpedo* used, the  $\alpha$ ,  $\beta$ ,  $\gamma$ , and/or  $\delta$  chains of the AcChR were labeled and cholinergic agonists enhanced their labeling (Oswald & Changeux, 1981a,b; Muhn & Hucho, 1983; Haring et al., 1983; Kaldany & Karlin, 1983; Heidmann et al., 1983). These data lead to the suggestion (Heidmann et al., 1983) that this unique "allosteric" site is common to all subunits and is located on the transmembrane axis of symmetry of the AcChR molecule where the distances to all five subunits are minimal.

We have recently shown that [ $^3\text{H}$ ]chlorpromazine ([ $^3\text{H}$ ]-CPZ) labels Ser-262 of AcChR  $\delta$  chain from *T. marmorata* via the high-affinity NCB site (Giraudat et al., 1986). In the present work, we sought to identify the residues labeled by [ $^3\text{H}$ ]CPZ in another subunit, the  $\beta$  chain. By sequence analysis of tryptic and CNBr peptides, we have identified two labeled residues in the  $\beta$  chain sequence that are located in a region homologous to that containing Ser-262 in the  $\delta$  chain. These findings suggest that, in both chains examined up to now, the same structural element, namely, the hydrophobic segment M II, is involved in the formation of the high-affinity NCB site and that this segment lies in the vicinity of the axis of symmetry of the AcChR molecule.

#### MATERIALS AND METHODS

**Materials.** Phencyclidine was a gift from A. Jaganathan (University Louis Pasteur, Strasbourg, France). [ $^3\text{H}$ ]CPZ (20–25 Ci/mmol) was purchased from New England Nuclear, carbamoylcholine chloride and unlabeled CPZ were from Sigma, TPCK-treated trypsin was from Worthington, and

CNBr was from Kodak. Live *T. marmorata* were provided by the Biological Station of Arcachon (France).

**Covalent Labeling of AcChR by [ $^3\text{H}$ ]CPZ.** Large batches (200 nmol of  $\alpha$ -toxin binding sites) of purified (Saitoh et al., 1980) and alkali-treated (Neubig et al., 1979) AcChR-rich membrane fragments were labeled by [ $^3\text{H}$ ]CPZ exactly as described (Giraudat et al., 1986). Final concentrations during UV irradiation were as follows: 5  $\mu\text{M}$   $\alpha$ -toxin binding sites, 1 mM carbamoylcholine, 2.5  $\mu\text{M}$  isotopically diluted [ $^3\text{H}$ ]CPZ (2–3 Ci/mmol), and when indicated, 200  $\mu\text{M}$  phencyclidine.

After illumination, the membranes were centrifuged and the pellets were solubilized in sample loading buffer (Laemmli, 1970) and submitted to preparative NaDodSO<sub>4</sub>/10% acrylamide/0.13% bis(acrylamide) gel electrophoresis (Devillers-Thiery et al., 1979).

**Purification of the  $\beta$  Chain.** Individual AcChR subunits were eluted from appropriate sections of preparative gels (Giraudat et al., 1986). After dialysis against water and lyophilization, purified chain was dissolved at 1 mg of protein/mL in 1% NaDodSO<sub>4</sub>, treated with dithiothreitol, and reacted with iodoacetic acid according to Allen (1981). Purified chain was then incubated for 24 h at 37 °C in the presence of 0.72 M dithiothreitol to reduce methionine sulf-oxides (Houghten & Li, 1983). After desalting (Giraudat et al., 1986), the  $\beta$  chain was precipitated twice with acetone.

The final material migrated as a single band on a polyacrylamide gel. Radioactivity incorporated into the polypeptide was measured as described (Oswald & Changeux, 1981a). The amount of protein was quantified by densitometric scanning of the Coomassie blue stained gel, with bovine serum albumin as a standard. The specific radioactivity of the purified  $\beta$  chain did not differ significantly from that just after irradiation (typically 2100–2500 cpm/ $\mu\text{g}$  of  $\beta$  chain vs. 450–750 cpm/ $\mu\text{g}$  of  $\beta$  chain for the phencyclidine-protected batch). The purified material represented approximately 50% of the original amount of  $\beta$  chain.

**Cleavage of the  $\beta$  Chain.** Trypsin digestion of the purified  $\beta$  chain was performed exactly as described (Giraudat et al., 1986). For CNBr cleavages, dry samples were dissolved (1 mg of protein/mL) in 70% formic acid and CNBr was added to a final concentration of 0.07 M. After 24 h at room temperature under nitrogen in the dark, an equal amount of CNBr was added and the reaction was allowed to proceed for a further 24-h period. The reaction mixture was then lyophilized.

**HPLC of Peptides.** A Waters HPLC system with a Valco injector and an Anacomp 220 (Kontron) data module was used. Tryptic and CNBr fragments were chromatographed on a Bu-300 Aquapore (Brownlee Labs) reversed-phase column (4.6  $\times$  220 mm) by using gradients of 0.1% trifluoroacetic acid in H<sub>2</sub>O (solvent A) and 0.1% trifluoroacetic acid in 60% 1-propanol/30% acetonitrile/10% H<sub>2</sub>O (solvent B). For injection, (i) dried samples were resolubilized in a minimal volume of formic acid and then diluted 5–10 times in the equilibrating solvent (usually 40% solvent B), or (ii) for re-purification, pooled fractions were diluted with solvent A up to starting conditions.

**Sequence Analysis.** Amino acid compositions were determined as described (Lederer et al., 1983). Automated Edman degradation was carried out in a Beckman 890 C spinning cup sequenator with 0.1 M Quadrol in the presence of Polybrene as described (Lederer et al., 1983) with the following modifications. The commercial Quadrol reagent (Pierce) was used as such, and peptides were dissolved in 66% formic acid for loading. The HPLC system used for identification of PTH-

Table I: Yields of PTH-Amino Acids upon Automated Edman Degradation of Tryptic- and CNBr-Derived Peptides<sup>a</sup>

| cycle                          | tryptic pools C + D <sup>b</sup> | tryptic, 65 min <sup>c</sup> |         | CNBr pool II <sup>d</sup> |         |                     |
|--------------------------------|----------------------------------|------------------------------|---------|---------------------------|---------|---------------------|
| 1                              | S                                | L (560)                      | W (160) | S (440) <sup>e</sup>      | I       | P (100)             |
| 2                              | D (1190)                         | F (1140)                     | H (240) | L (440)                   | N (120) | S (50) <sup>e</sup> |
| 3                              | D (1340)                         | S                            | L (300) | S (230) <sup>e</sup>      | Q (140) | Y (90)              |
| 4                              | P (900)                          | E (640)                      | D (230) | I (390)                   | D (70)  | E (100)             |
| 5                              | S                                |                              | G (90)  | S (240) <sup>e</sup>      | A (130) | D (130)             |
| 6                              | Y (1080)                         | K (120)                      | L (60)  | A (270)                   | F (90)  |                     |
| 7                              | E (530)                          | W (180)                      |         | L (270)                   | T (70)  | T (70)              |
| 8                              | D (620)                          | H (250)                      |         | L (230)                   | E (30)  | F (100)             |
| 9                              |                                  | L (260)                      |         | A (150)                   |         | Y (50)              |
| 10                             | T (500)                          | D (170)                      |         |                           |         | L (150)             |
| 11                             | F (750)                          | G (150)                      |         | T (130)                   |         | I (40)              |
| 12                             | Y (560)                          | L (250)                      |         |                           |         |                     |
| 13                             | L (400)                          | T (80)                       |         | F (140)                   |         |                     |
| 14                             | I (730)                          | Q (100)                      |         | L (140)                   |         |                     |
| 15                             |                                  |                              |         | L (90)                    |         |                     |
| 16                             | Q (370)                          |                              |         |                           |         |                     |
| 17                             | R (290)                          |                              |         |                           |         |                     |
| 18                             | K (200)                          |                              |         |                           |         |                     |
| 19                             | P (320)                          |                              |         |                           |         |                     |
| 20                             | L (280)                          |                              |         |                           |         |                     |
| 21                             | F (400)                          |                              |         |                           |         |                     |
| repetitive yield (%)           | 92                               | 85                           | 76      | 89                        | 79      | 90                  |
| initial amount (pmol)          | 1340                             | 810                          | 360     | 550                       | 230     | 140                 |
| starting position <sup>f</sup> | 199                              | 380                          | 386     | 250                       | 175     | 202                 |

<sup>a</sup> For each sequence analysis the PTH-amino acids identified are designated by the conventional one-letter abbreviations, and their yields in picomoles are given in parentheses. For lack of a reliable calibration standard, PTH-Ser could not be quantified. For each identified sequence, the apparent repetitive yield and initial amount of sequence were calculated by linear regression analysis. <sup>b</sup> Material contained in pools C and D of Figure 1 was mixed. The sample loaded contained 33 000 cpm. <sup>c</sup> Nonradioactive material contained in the major  $A_{210}$  peak eluting at 65 min in Figure 1. Asp was identified at position 389 (cycles 10 and 4) in place of the Asn in *T. californica*. <sup>d</sup> Repurified material contained in pool II of Figure 2. The sample loaded contained 70 000 cpm. In this particular analysis, isoleucine could not be quantified at cycle 1 but was actually quantified upon sequence analysis of pools III and IV. <sup>e</sup> In this analysis the amounts of identified PTH-Ser are given on an arbitrary scale (see above), only to illustrate the relative amounts released at various cycles. <sup>f</sup> For each identified sequence, the position of the amino-terminal residue in the complete sequence of  $\beta$  chain is given.

amino acids consisted of two Waters Model 510 pumps, a Waters WISP 710 B automatic injector, and a Kratos 773 spectrophotometer operated at 0.001 AUFS. The complete system was actuated by a Waters 840 data and control station.

## RESULTS

**Labeling of the  $\beta$  Chain by [<sup>3</sup>H]CPZ.** Large batches of AcChR-rich membrane fragments (200 nmol of  $\alpha$ -toxin binding sites) were photolabeled by [<sup>3</sup>H]CPZ under equilibrium conditions in the presence of 1 mM carbamoylcholine. Analytical polyacrylamide gel electrophoresis of [<sup>3</sup>H]CPZ-labeled membranes confirmed that, as originally shown by Oswald and Changeux (1981b), all AcChR chains were labeled. In the presence of unlabeled phencyclidine, a specific ligand for the high-affinity NCB site, the incorporation of [<sup>3</sup>H]CPZ into all AcChR chains was decreased (by 70–75% in the case of  $\beta$  chain) (Oswald & Changeux, 1981b; Heidmann et al., 1983).

The AcChR  $\beta$  chains derived from membranes labeled in the absence or presence of the noncompetitive blocker phencyclidine were purified by preparative polyacrylamide gel electrophoresis with no detectable loss of covalently bound [<sup>3</sup>H]CPZ (see Materials and Methods). Determination of the specific radioactivity (see Materials and Methods) of the purified material indicated that approximately 4% of the  $\beta$  chain molecules were labeled by [<sup>3</sup>H]CPZ in a phencyclidine-sensitive manner. This value reflects both the distribution of label among the five subunits via the unique high-affinity NCB site and incomplete labeling (approximately 15%) of the available NCB sites.

**Analysis of  $\beta$  Chain Tryptic Fragments.** A preliminary localization of the labeled residues in the  $\beta$  chain sequence was obtained by analysis of tryptic fragments. Fractionation of the total tryptic digest of purified  $\beta$  chain by reversed-phase

Table II: Results of Sequence Analysis of [<sup>3</sup>H]CPZ Specifically Labeled Tryptic Peptides from  $\beta$  Chain<sup>a</sup>

| pool  | minimal estimate of amount of peptide loaded <sup>b</sup> (pmol) | amount of identified sequence <sup>c</sup> (pmol) |
|-------|--|---|
| A     | 420  | 540   |
| B     | 500  | 510   |
| C + D | 380  | 1340  |
| E     | 80   | 320   |

<sup>a</sup> Material contained in the various pools shown in Figure 1 was subjected to automated sequence analysis. <sup>b</sup> For each sample analyzed, a minimal estimate of the amount of peptide loaded having the same sequence as the radiolabeled fragment was calculated by dividing the quantity of radioactivity loaded by the specific radioactivity of the uncut  $\beta$  chain used (phencyclidine-sensitive labeling: 86 000 cpm/nmol of  $\beta$  chain). <sup>c</sup> For each sample, the same unique amino-terminal sequence was identified. The extrapolated initial amount of this sequence was calculated by linear regression analysis of the data.

HPLC produced the chromatogram shown in Figure 1. The recovery of the injected radioactivity in this analysis was 75%. Approximately 10% of the injected radioactivity was present in the unbound material; however, this first radioactive peak was not reduced in the phencyclidine-protected batch and was not analyzed further.

The majority (60%) of the recovered phencyclidine-sensitive labeling was present in a broad radioactive peak eluted between 105 and 125 min. This material was subdivided into five pools (see legend to Figure 1) corresponding to the distinct peaks of UV-absorbing material. Repurification of these pools (A–E) yielded the five distinct peaks shown in the lower part of Figure 1. Upon automated sequence analysis of each of these samples, however, the same unique amino-terminal sequence was observed; the results of the most extended analysis are shown in Table I. Comparison with the known primary structure

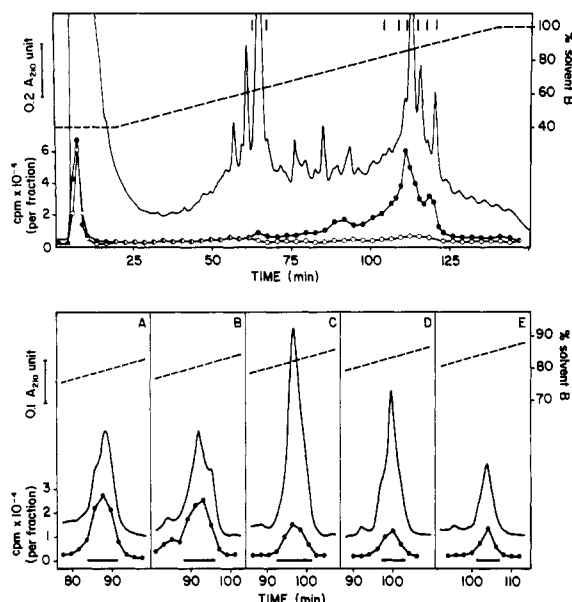


FIGURE 1: Fractionation of tryptic peptides from [ $^3\text{H}$ ]CPZ-labeled  $\beta$  chain by reversed-phase HPLC. (Upper panel) Purified labeled  $\beta$  chain (8 nmol) was incubated with trypsin. The dried digest was dissolved in formic acid and applied to a  $\text{C}_4$  column equilibrated in 40% solvent B (see Materials and Methods). Elution was carried out at 0.5 mL/min with a gradient of solvent B as indicated by the broken line. The eluate was monitored by absorbance at 210 nm (solid line). Radioactivity contained in the fractions ( $\bullet$ ) collected at 1.5-min intervals was measured by subjecting aliquots (7.5  $\mu\text{L}$ ) to liquid scintillation counting. Parallel treatment of  $\beta$  chain labeled by [ $^3\text{H}$ ]CPZ in the presence of phencyclidine produced a similar  $A_{210}$  profile (not shown) and the radioactivity profile shown here ( $\circ$ ). The vertical bars delimit the pools of fractions taken for repurification. (Lower panel) Five pools of fractions were made, which contained respectively the material eluting between 104.5 and 109 min (pool A), 109 and 112 min (B), 112 and 115 min (C), 115 and 118 min (D), and 118 and 121 min (E). Each of them was subjected to two additional HPLC steps as above, but a lower gradient slope (0.33% solvent B/min) was used. The relevant portions of the radioactivity ( $\bullet$ ) and optical density profiles (solid line) of the last HPLC runs are shown here. In each case, the horizontal bars indicate the material subsequently characterized by sequence analysis.

of AcChR  $\beta$  chain from *T. californica* (Noda et al., 1983a) indicates that this sequence (Ser-Asp-Asp-Pro-Ser-Tyr-Glu-Asp-Xaa-Thr-Phe-Tyr-Leu-Ile-Xaa-Gln-Arg-Lys-Pro-Leu-Phe) corresponds to a tryptic fragment extending from Ser-199 (cleavage at Arg-198). As shown in Table II, upon analysis of each pool the quantity of radioactivity loaded in the sequenator was sufficient to ensure that the amount of the corresponding peptide present was above the detection limit for PTH-amino acids. The unique identified amino-terminal sequence thus corresponds to the labeled fragment. In every case, no release of radioactivity was observed at any of the up to 21 cycles performed, indicating that [ $^3\text{H}$ ]CPZ was incorporated C-terminal to Phe-219.

It is apparent from the data presented in Table II that the ratio between the estimated amount of peptide loaded and the actual amount of identified sequence is not constant for all peptide pools. This observation suggests that the [ $^3\text{H}$ ]CPZ-labeled peptides may not have coeluted exactly with the unlabeled peptides of the same sequence (see Discussion).

The nonradioactive material contained in the major  $A_{210}$  peak eluting at 65 min (Figure 1) was also characterized. After repurification in the same HPLC conditions, it was subjected to sequence analysis and found to be composed of a major fragment extending from residue Leu-380 and a minor one extending from Trp-386 (Table I). This fraction was also submitted to amino acid analysis. The observed composition

Table III: Comparison of Experimentally Determined Amino Acid Composition of Unlabeled Material Eluting at 65 min with That Predicted for  $\beta$  Subunit Fragments

|            | $x^a$ | $\beta$ 380-409 <sup>b</sup> | $\beta$ 380-425 | $\beta$ 380-437 | $\beta$ 380-469 |
|------------|-------|------------------------------|-----------------|-----------------|-----------------|
| Cys        | 0.054 | 0.27 (0)                     | 0.38 (0)        | 0.38 (0)        | 0.54 (1)        |
| Asx        | 0.992 | 4.96 (2)                     | 6.95 (4)        | 6.95 (6)        | 9.92 (10)       |
| Thr        | 0.211 | 1.05 (2)                     | 1.48 (2)        | 1.48 (2)        | 2.11 (3)        |
| Ser        | 0.647 | 3.23 (1)                     | 4.53 (3)        | 4.53 (3)        | 6.47 (6)        |
| Glx        | 1.009 | 5.05 (5)                     | 7.07 (9)        | 7.07 (10)       | 10.10 (10)      |
| Pro        | 0.495 | 2.47 (2)                     | 3.47 (2)        | 3.47 (2)        | 4.95 (5)        |
| Gly        | 0.404 | 2.02 (1)                     | 2.83 (1)        | 2.83 (1)        | 4.04 (2)        |
| Ala        | 0.810 | 4.05 (2)                     | 5.67 (4)        | 5.67 (6)        | 8.10 (8)        |
| Val        | 0.549 | 2.74 (2)                     | 3.84 (2)        | 3.84 (4)        | 5.49 (7)        |
| Met        | 0.273 | 1.36 (1)                     | 1.91 (1)        | 1.91 (2)        | 2.73 (2)        |
| Ile        | 0.606 | 3.03 (1)                     | 4.24 (2)        | 4.24 (2)        | 6.06 (5)        |
| Leu        | 1     | 5 (5)                        | 7 (7)           | 7 (7)           | 10 (10)         |
| Tyr        | 0.300 | 1.5 (0)                      | 2.1 (1)         | 2.1 (2)         | 3.00 (3)        |
| Phe        | 0.661 | 3.30 (1)                     | 4.63 (2)        | 4.63 (2)        | 6.61 (8)        |
| His        | 0.196 | 0.98 (1)                     | 1.37 (1)        | 1.37 (1)        | 1.96 (2)        |
| Lys        | 0.497 | 2.45 (3)                     | 3.48 (4)        | 3.48 (5)        | 4.97 (5)        |
| Arg        | 0.145 | 0.72 (0)                     | 1.01 (0)        | 1.01 (1)        | 1.45 (1)        |
| $\Delta^c$ |       | 14.24                        | 11.97           | 7.48            | 3.34            |

<sup>a</sup> Material contained in the major  $A_{210}$  peak eluting at 65 min in Figure 1 was subjected to amino acid composition analysis. The amounts of each amino acid are normalized to Leu = 1 mol/mol; values shown here are the average of two analyses. <sup>b</sup> For each fragment of the  $\beta$  chain considered here, the values in parentheses denote the number of residues present in the peptide as predicted from the known sequence of  $\beta$  chain from *T. californica*. For comparison, the results of the experimental amino acid composition analysis are shown normalized to the number of Leu residues predicted for the peptide. <sup>c</sup> This index is the sum, for all the amino acids, of the percentage of difference between predicted and experimental values. A better fit corresponds to a lower value of  $\Delta$ , and a perfect fit to  $\Delta = 0$ . This index is not artifactually decreasing simply by increasing the length of the fragment considered; for instance, the fragment  $\beta$  350-469 yields to  $\Delta = 5.01$ .

was compared to those predicted for tryptic peptides extending from Leu-380 to the various Lys/Arg residues down to the C-terminus, by use of the known sequence from *T. californica* (Table III). For each fragment, predicted and experimental values were compared for individual amino acids and a quantitative estimation of the overall fit was expressed by the  $\Delta$  index. The best fit was obtained for a fragment extending to the C-terminus of the chain.

**Analysis of  $\beta$  Chain CNBr Fragments.** Fractionation of the total CNBr digest of purified  $\beta$  subunit produced the chromatogram shown in Figure 2. Approximately 15% of the injected radioactivity was recovered in the unbound material, while 70% of injected radioactivity, including all the phencyclidine-sensitive labeling, eluted between 45% and 90% solvent B.

Four pools of fractions containing the specifically labeled material were characterized further. Pool I contained the material eluting between 30 and 50 min, which represented 10% of the phencyclidine-sensitive labeling. The material eluting between 74 and 110 min, together with a large  $A_{210}$  peak, represented 70% of the phencyclidine-sensitive labeling. This region was subdivided into pools II, III, and IV (see legend to Figure 2). The radioactivity contained in each of the four pools was decreased by 85-90% in material labeled in the presence of phencyclidine. Each of these pools was refractionated in the same HPLC system, as illustrated in the lower part of Figure 2, and then characterized by automated sequence analysis.

Each of the pools II-IV was found to contain a mixture of the same three amino-terminal sequences; the results obtained for pool II are shown in Table I. Amino acids were assigned to each peptide on the basis of homology with the known sequence of *T. californica*  $\beta$  chain (Noda et al., 1983a). The

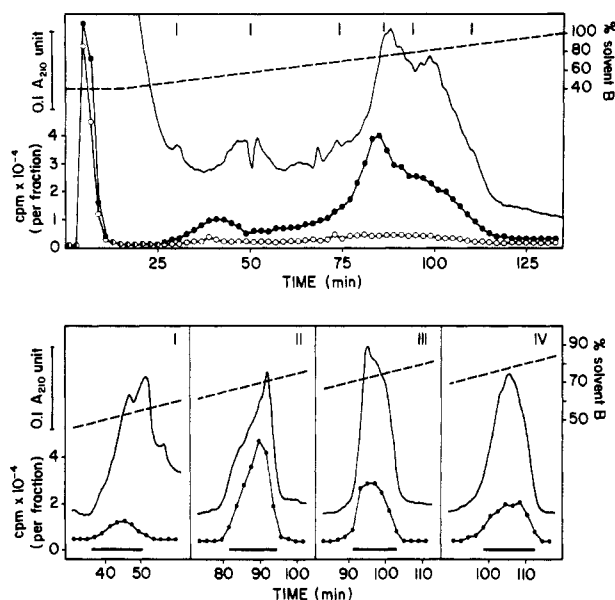


FIGURE 2: Fractionation of CNBr peptides from  $[^3\text{H}]\text{CPZ}$ -labeled  $\beta$  chain by reversed-phase HPLC. (Upper panel) Purified  $[^3\text{H}]\text{CPZ}$ -labeled  $\beta$  chain (8 nmol) was cleaved with CNBr and the total digest analyzed by reversed-phase HPLC as in Figure 1. The solid line represents absorbance at 210 nm. Aliquots (20  $\mu\text{L}$ ) of the fractions collected at 2-min intervals were subjected to liquid scintillation counting ( $\bullet$ ). Parallel treatment of  $\beta$  chain labeled by  $[^3\text{H}]\text{CPZ}$  in the presence of phencyclidine produced a similar  $A_{210}$  profile (not shown) and the radioactivity profile shown here ( $\circ$ ). The vertical bars delimit the pools of fractions taken for repurification. (Lower panel) Four pools of fractions from the upper chromatogram were made, which contained respectively the material eluting between 30 and 50 min (pool I), 74 and 86 min (II), and 86 and 94 min (III), and 94 and 110 min (IV). Each of them was subjected to an additional HPLC step as above. The relevant parts of the radioactivity and optical density profiles are shown here. The horizontal bars indicate the material subsequently subjected to sequence analysis.

sequence Ser-Leu-Ser-Ile-Ser-Ala-Leu-Leu-Ala-Xaa-Thr... corresponded to a peptide extending from Ser-250 (CNBr cleavage at Met-249). The sequence Pro-Ser-Tyr-Glu-Asp-Xaa-Thr-Phe-Tyr-Leu-Ile... corresponded to a peptide extending from Pro-202, presumably reflecting acid cleavage of the peptide bond between Asp-201 and Pro-202 (Allen, 1981). The sequence Ile-Asn-Gln-Asp-Ala-Phe-Thr-Glu... corresponded to a peptide extending from Ile-175, except that Gln was clearly identified at position 177 in place of the Lys in *T. californica*. Furthermore, we have to assume that residue 174 is Met in *T. marmorata*, instead of Val as in *T. californica*, to account for the fact that this peptide was generated by CNBr cleavage. Such species-specific mutations have already been noted between the AcChR  $\alpha$  chains (Devillers-Thiéry et al., 1983) and  $\delta$  chains (Giraudat et al., 1986) from these two *Torpedo* species.

A clear release of radioactivity was observed at sequence cycles 5 and 8 for all three samples; the detailed data for pool II are shown in Figure 3 (see also Figure 4). We tried to estimate whether this release of radioactivity could have originated from a minor sequence that had escaped identification at the PTH-amino acids level. As calculated from the phencyclidine-sensitive labeling of the uncut  $\beta$  chain used here (80 000 cpm/nmol of  $\beta$  chain), the amount of radioactivity recovered at cycles 5 and 8 corresponded, in the case of pool II, to the presence of at least 100 and 40 pmol, respectively, of corresponding peptide at these cycles. This is clearly an underestimate because, as multiple residues of the  $\beta$  chain are labeled, the specific radioactivity at a given residue is less than that of the total chain. In any case these minimal values are

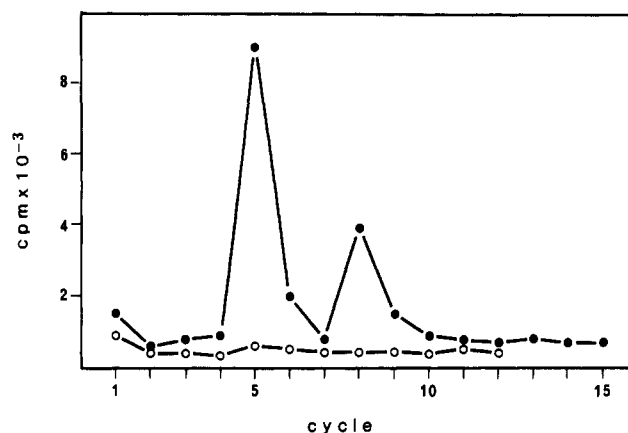


FIGURE 3: Radioactivity released upon sequence analysis of CNBr peptides contained in pool II. Repurified material contained in pool II of Figure 2 was subjected to automated sequence analysis. The amount of radioactivity found associated with the PTH fraction at each cycle is shown ( $\bullet$ ). The sample loaded contained 70 000 cpm, which correspond to approximately 35 000 cpm of effectively sequenced material (assuming an initial yield of about 50% for Edman degradation, the average value routinely observed in this laboratory). By correction of the data for the repetitive yield (89%) calculated from the PTH data of this analysis (Table I), the radioactivity recovered at cycles 5 and 8 accounts for approximately 60% [ $8200/(0.89)^5 + 3100/(0.89)^8 = 22\,500$  cpm] of the theoretical maximum. The radioactivity released upon sequencing of unfractionated material contained in pools II–IV derived from phencyclidine-protected  $\beta$  chain is also shown ( $\circ$ ). The three amino-terminal sequences described for the unprotected material were observed with this phencyclidine-protected sample and were present in approximately equimolar amounts (360 pmol of each) (data not shown).

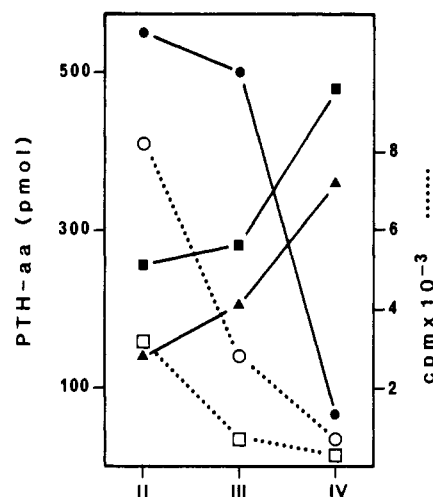


FIGURE 4: Comparison of the sequence results of CNBr peptides from pools II, III, and IV. Upon sequence analysis, pools II–IV of Figure 2 were found to contain a mixture of three amino-terminal sequences (see text). The initial amount of each sequence was determined by linear regression analysis of the yields for the relevant PTH derivatives. For each pool of peptides (II–IV), the initial amounts of sequences extending from Ser-250 ( $\bullet$ ), Pro-202 ( $\blacktriangle$ ), or Ile-175 ( $\blacksquare$ ) (solid lines) and the radioactivity released over background level at sequence cycle 5 ( $\circ$ ) or 8 ( $\square$ ) (dotted lines) are represented.

above the detection limit for PTH-amino acids. A similar calculation leads to the same conclusion in the case of pool III. For pools II and III, and by extension for pool IV, the sequence corresponding to the labeled peptide(s) was thus among the three identified sequences.

Comparison of the sequence results obtained for CNBr peptides in pools II–IV demonstrates that the three identified amino-terminal sequences were not uniformly distributed between these pools. As shown in Figure 4, the amount of the sequences extending from Ile-175 and from Pro-202 pro-

gressively increased from pool II to pool IV, whereas the sequence extending from Ser-250 decreased from pool II to pool IV. The quantity of radioactivity released at each of cycles 5 and 8 followed the relative distribution of this last sequence; this clearly points to Ser-254 and Leu-257 as sites of incorporation of [ $^3\text{H}$ ]CPZ.

Labeling of these particular residues was inhibited by phencyclidine, as shown by sequence analysis of CNBr peptides purified in parallel from  $\beta$  chain labeled in the presence of phencyclidine. The unfractionated material corresponding to pools II–IV consisted of a mixture of the three amino-terminal sequences described above, but no radioactivity was released at cycles 5 or 8 (Figure 3).

In the case of pool I, no amino-terminal sequence could be reliably identified because of the insufficient amount of material. However, a small but significant release of radioactivity was observed at cycles 5 and 8 (data not shown). It is thus most likely that the sequence extending from Ser-250 was present in pool I as well and was responsible for the radioactivity released.

## DISCUSSION

Since the elucidation of the complete primary structure of the AcChR, several attempts have been made to localize ligand binding sites and to characterize the folding of the various polypeptide subunits in the functional oligomer. One approach involves the covalent labeling of functionally significant binding sites and the identification of the modified amino acids by protein chemical techniques [see, e.g., Kao et al. (1984) and Giraudat et al. (1986)]. Reversible interactions of the non-competitive blocker CPZ with AcChR-rich membranes have been characterized in detail (Heidmann et al., 1983). Upon UV irradiation, selective labeling of the four AcChR chains from *T. marmorata* occurs in the presence of cholinergic agonists under conditions of occupancy of the high-affinity NCB site (Oswald & Changeux, 1981b; Heidmann et al., 1983). CPZ thus offers the opportunity to prove the structure of this site and, in addition, to assess the degree of symmetry of the AcChR molecule at its level.

The extent of covalent incorporation of [ $^3\text{H}$ ]CPZ into a given AcChR chain is quite low and reflects both the yield of the photolabeling reaction and the fact that the labeling is distributed among the five subunits. In addition, covalent labeling was carried out by using nonsaturating concentrations of CPZ in order to provide an optimal signal-to-noise ratio for labeling of the high-affinity site. As a result, it was impractical to purify and characterize the radioactive peptides themselves, which were rather used as tracers for the unlabeled peptides of the same sequence. This consideration imposed some technical constraints, in particular to ensure that the labeled peptides and their nonlabeled counterparts would comigrate during the peptide separation procedures. We therefore avoided generating too small peptide fragments, as their behavior on reversed-phase HPLC was expected to be more affected by the addition of a molecule as large as CPZ. Comparison of the optical density and radioactivity profiles in Figures 1 and 2 suggests that even with the long trypsin- and CNBr-derived peptides used here, the specifically labeled peptides eluted slightly earlier than their nonlabeled counterparts, possibly as a result of the positive charge carried by CPZ. Such a slight shift in elution position could account for the observations that the ratio of the amount of identified sequence to the amount of radioactivity loaded in the sequenator increases from pool A to pool E of tryptic peptides (Table II) and that the ratio of the amount of identified sequence starting at Ser-250 to the amount of released radio-

activity is higher in pool III than in pool II for the CNBr-derived peptides (Figure 4).

The specifically labeled peptides generated by trypsin or CNBr cleavage of the  $\beta$  chain displayed a marked hydrophobic character. However, the HPLC conditions used here (a large-pore C4 column and a high initial percentage of organic solvent) provided a satisfactory recovery of the radioactive material. Despite the use of chromatographic conditions recommended for separation of large hydrophobic peptides [e.g., Taar and Crabb (1983)], we were unable to purify to homogeneity the various CNBr fragments present in pools II–IV. The radioactivity released at cycles 5 and 8 on sequence analysis of these pools could a priori have originated from any of the three identified  $\beta$  chain fragments present. The candidates as labeled residues were thus as follows: Ala-179, Asp-206, and Ser-254 (cycle 5) and Glu-182, Phe-209, and Leu-257 (cycle 8) (see Figure 5A). The difference in abundance of the three sequences between the various pools, however, enabled us to relate the release of radioactivity at both sequence cycle 5 and sequence cycle 8 to the presence of the amino-terminal sequence extending from Ser-250. Sequence analysis of tryptic peptides provided independent and convergent evidence for the identification of Ser-254 and Leu-257 as labeled residues. The sequence results for tryptic pools A–E indeed directly demonstrated that residues Asp-206 and Phe-209 were not labeled. Furthermore, the fact that 60% of the phencyclidine-sensitive labeling was contained in the sequenced tryptic peptides starting at Ser-199 also tends to exclude Ala-179 and Glu-182 as sites of labeling (see Figure 5A).

Purification and sequence analysis of material derived from the control batch of  $\beta$  chain unambiguously demonstrated that labeling of residues Ser-254 and Leu-257 was protected by phencyclidine. These residues thus lie within or in close proximity to the unique high-affinity NCB binding site.

Because of the technical constraints mentioned above, it proved impossible to explore in a systematic way if other residues of the  $\beta$  chain were also specifically labeled by [ $^3\text{H}$ ]CPZ. Under the conditions used here for HPLC, hydrophilic peptides most probably eluted with unbound material which did not contain phencyclidine-sensitive labeling. Any additional specifically labeled residues, if they exist, could thus be located only in the unsequenced parts of the hydrophobic domains of the  $\beta$  chain.

Unlabeled tryptic fragments starting at Leu-380 and Trp-386 were identified in this study. The results of amino acid composition analysis suggested that this tryptic material extended to the C-terminus of the  $\beta$  chain (Table III). Accordingly, these peptides included the amphipathic helix A and the hydrophobic segment M IV (see Figure 5A). Their behavior in the HPLC system used here is compatible with the hydrophobic character predicted for such a sequence. The amphipathic helix A, which has been proposed in some models (Guy, 1984; Finer-Moore & Stroud, 1984) as a potential ion channel component, thus does not appear to be labeled by [ $^3\text{H}$ ]CPZ.

Residues Ser-254 and Leu-257 are located in the hydrophobic segment M II of the  $\beta$  subunit. The observation that the neighboring residues were not labeled by [ $^3\text{H}$ ]CPZ, in addition to providing an internal control for the selectivity of CPZ labeling, is consistent with the proposed  $\alpha$ -helical arrangement of segment M II. In such a configuration, the labeled residues Ser-254 and Leu-257 would be separated by about one helical turn and would be aligned on one face of the vertical axis (Figure 5B). This face of the  $\alpha$ -helix might



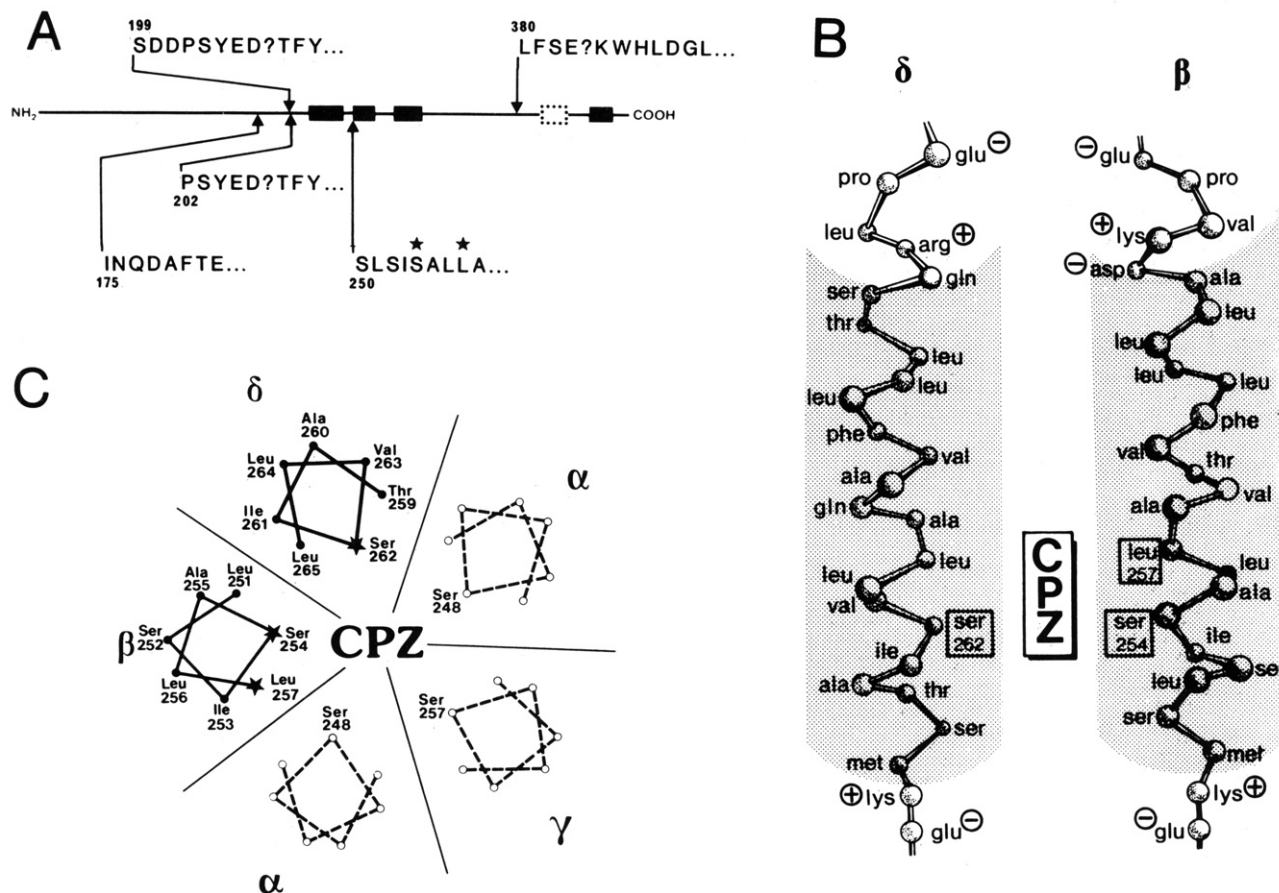


FIGURE 5: (A) Location of sequenced peptides within the  $\beta$  chain primary structure. Schematic drawing of the  $\beta$  chain. Black boxes indicate the four hydrophobic segments (M I-M IV), and the open box indicates amphipathic helix A. Identified tryptic and CNBr peptides are indicated above and below, respectively, and localized along the sequence of the  $\beta$  chain from *T. californica*. [<sup>3</sup>H]CPZ-labeled residues are marked with an asterisk. (B) Position of [<sup>3</sup>H]CPZ-labeled residues in the M II segments of the  $\beta$  and  $\delta$  chains. In this cartoon the M II segments of the  $\beta$  and  $\delta$  chains are depicted as transmembrane  $\alpha$ -helices. Charged residues are indicated. Identified residues labeled by [<sup>3</sup>H]CPZ in a phencyclidine-sensitive manner are framed. (C) Schematic model of the proposed organization of the M II segments from the several AcChR subunits within the  $\alpha_2\beta\gamma\delta$  oligomer. The subunits are arranged around a transmembrane axis of 5-fold symmetry in the order suggested by Karlin et al. (1983). Segments M II are organized in transmembrane  $\alpha$ -helices. Only a portion of each segment M II is represented here, viewed from the axis of the helix. This helical-wheel diagram indicates the positions of the  $\alpha$ -carbons of the amino acids but does not make specific assumptions about the locations of their side chains. The helices have been oriented in such a way that, in the  $\beta$  and  $\delta$  chains, the identified sites of labeling by CPZ (indicated by stars) are exposed toward the central axis of symmetry of the molecule, assumed here to be perpendicular to the plane of the figure. In the  $\alpha$  and  $\gamma$  chains, the serine residues homologous to the CPZ-labeled  $\beta$  Ser-254 and  $\delta$  Ser-262 are shown.

be selectively accessible to CPZ bound to the high-affinity NCB site (see model in Figure 5C).

Upon alignment of the primary structures of the four AcChR chains from *T. californica* to optimize sequence homologies (Noda et al., 1983b), residue Ser-254 of the  $\beta$  chain coincides with Ser-262 of the  $\delta$  chain. This last residue has been previously demonstrated to be specifically labeled by [<sup>3</sup>H]CPZ (Giraudat et al., 1986). These results provide experimental evidence that, at least for the two chains analyzed so far, homologous regions of the AcChR subunits are involved in the formation of the high-affinity NCB site (see Figure 5B,C). All four chains display high sequence homology in this domain; in particular, both  $\alpha$  and  $\gamma$  chains also contain a Ser residue at the position corresponding to  $\beta$  Ser-254 and  $\delta$  Ser-262. The attractive hypothesis that these Ser residues are also specifically labeled by [<sup>3</sup>H]CPZ remains, however, to be experimentally tested.

The second labeled residue identified here in the  $\beta$  chain (Leu-257) corresponds upon sequence alignment to Leu-265 of the  $\delta$  chain, which is not labeled by [<sup>3</sup>H]CPZ (Giraudat et al., 1986). Despite an apparent degree of symmetry, some subtle differences thus seem to exist between the respective contributions of the various AcChR chains to the NCB site, as already suggested by the variability in the labeling patterns

obtained, depending on the ligand or on the species of *Torpedo* used [see Haring et al. (1983)].

As discussed by Heidmann et al. (1983), the most plausible interpretation of reversible binding and covalent labeling studies is that the unique high-affinity NCB site is located on the central axis of symmetry, where the distance between all five subunits is at a minimum. According to this model, our present results suggest that for each subunit the hydrophobic segment M II would lie close enough to the central axis of symmetry and be oriented so as to render residues  $\beta$  254,  $\beta$  257, and  $\delta$  262 accessible to CPZ (Figure 5C).

Rapid-mixing photolabeling experiments have shown that CPZ labeling of the high-affinity NCB site occurs several orders of magnitude faster under conditions where the channel is open than when it is closed. The characteristics of this rapid labeling process support the notion that under these conditions CPZ binds to the AcChR without restriction to diffusion and covalently reacts with the subunits while the channel is open (Heidmann & Changeux, 1984, 1986). Despite the fact that the kinetics of covalent attachment of other NCBs such as quinacrine azide might be different (Cox et al., 1985), the above scheme is consistent with models based on electrophysiological recordings [review in Neher and Steinbach (1978) and Adams (1981)] which propose that some NCBs may,

under defined conditions, block the permeability response by entering the open channel in a diffusion-controlled manner and inhibiting ion flux by steric hindrance [see Changeux et al. (1986)].

In the present study, labeling by CPZ was carried out at equilibrium, in the presence of agonist, under conditions that favor the desensitized state of the AcChR in which the ion channel is closed (Heidmann et al., 1983). It is unclear at present to what extent the conformation of the high-affinity NCB site varies with the functional state of the AcChR and whether or not the covalent labeling by CPZ would reflect such structural changes. This question can be addressed by comparing the amino acids labeled by CPZ at equilibrium as in the present study with those labeled under conditions of rapid mixing where the ion channel is open.

In any case, the present results are consistent with the hypothesis that the hydrophobic segment M II, which at least in  $\beta$  and  $\delta$  chains is labeled by CPZ at equilibrium via the high-affinity NCB site, is directly linked to the ion channel and might even be one of its components (Giraudat et al., 1986). In agreement with this interpretation, Mishina et al. (1985) observed that deletion of  $\alpha$  249–257, which covers part of segment M II in the  $\alpha$  subunit, abolishes the ionic response without altering the apparent binding affinity for AcCh. In that study, however, a similar effect was also observed by deleting many other portions of the  $\alpha$  chain. It is also noteworthy that, from the sequence data presently available, segment M II is the most conserved domain of the AcChR subunits throughout phylogeny [see Stroud and Finer-Moore (1985)]. This argues in favor of an essential role of this domain in AcChR function.

#### ADDED IN PROOF

Since this paper was submitted, two reports from the same laboratory have appeared dealing with the localization of amino acid residues labeled by the photolabile noncompetitive blocker [ $^3\text{H}$ ]triphenylmethylphosphonium. Oberthür et al. (1986) identified the residue labeled by this compound on the  $\delta$  subunit as Ser-262, a residue previously shown in this laboratory by Giraudat et al. (1986) to be labeled by [ $^3\text{H}$ ]chlorpromazine. Then Hucho et al. (1986) reported evidence suggesting that residues homologous to  $\delta$  Ser-262 were labeled on the  $\alpha$  and  $\beta$  subunits. However, neither the amino acid sequence of the labeled peptides nor the specificity of the labeling at the amino acid level was reported. Despite the fact that specific covalent labeling by triphenylmethylphosphonium has been reported to occur only on the  $\beta$  and  $\delta$  chains (Muhn & Hucho, 1983; Oberthür et al., 1986) and that the number of binding sites per molecule of receptor has not been determined, these findings seem consistent with the experimental data presented here which support the original proposal (Heidmann et al., 1983) that the unique high-affinity NCB site is delimited by homologous regions of the five subunits.

More recently, Imoto et al. (1986) reported additional evidence that segment M II is a potential element of the ion channel. These authors, using a combination of site-directed mutagenesis and electrophysiological techniques, showed that a region of the  $\delta$  subunit comprising segment M II and the bend portion between segments M II and M III contributes to the regulation of the rate of ion transport through the open channel at low extracellular  $\text{Ca}^{2+}$  concentration.

#### ACKNOWLEDGMENTS

We thank S. Cortial for performing the amino acid analysis, Dr. A. Jaganathan for phencyclidine, and Dr. A. Klarsfeld for helpful comments.

#### REFERENCES

- Adams, P. R. (1981) *J. Membr. Biol.* 58, 161–174.
- Allen, G. (1981) *Sequencing of Proteins and Peptides*, Elsevier, Amsterdam.
- Anholt, R., Lindstrom, J., & Montal, M. (1985) *Enzymes Biol. Membr.* 3, 335–401.
- Changeux, J.-P., Devillers-Thiéry, A., & Chemouilli, P. (1984) *Science (Washington, D.C.)* 225, 1335–1345.
- Changeux, J.-P., Pinset, C., & Ribera, A. B. (1986) *J. Physiol. (London)* 378, 497–513.
- Claudio, T., Ballivet, M., Patrick, J., & Heinemann, S. (1983) *Proc. Natl. Acad. Sci. U.S.A.* 80, 1111–1115.
- Cox, R. N., Kaldany, R. R. J., Di Paola, M., & Karlin, A. (1985) *J. Biol. Chem.* 260, 7186–7193.
- Devillers-Thiéry, A., Changeux, J.-P., Paroutaud, P., & Strosberg, A. D. (1979) *FEBS Lett.* 104, 99–105.
- Devillers-Thiéry, A., Giraudat, J., Bentaboulet, M., & Changeux, J.-P. (1983) *Proc. Natl. Acad. Sci. U.S.A.* 80, 2067–2071.
- Finer-Moore, J., & Stroud, R. M. (1984) *Proc. Natl. Acad. Sci. U.S.A.* 81, 155–159.
- Giraudat, J., Montecucco, C., Bisson, R., & Changeux, J.-P. (1985) *Biochemistry* 24, 3121–3127.
- Giraudat, J., Dennis, M., Heidmann, T., Chang, J. Y., & Changeux, J.-P. (1986) *Proc. Natl. Acad. Sci. U.S.A.* 83, 2719–2723.
- Guy, H. R. (1984) *Biophys. J.* 45, 249–261.
- Haring, R., Kloog, Y., Kalir, A., & Sokolovsky, M. (1983) *Biochem. Biophys. Res. Commun.* 113, 723–729.
- Heidmann, T., & Changeux, J.-P. (1984) *Proc. Natl. Acad. Sci. U.S.A.* 81, 1897–1901.
- Heidmann, T., & Changeux, J.-P. (1986) *Biochemistry* 25, 6109–6113.
- Heidmann, T., Oswald, R. E., & Changeux, J.-P. (1983) *Biochemistry* 22, 3112–3127.
- Houghten, R. A., & Li, C. H. (1983) *Methods Enzymol.* 91, 549–559.
- Hucho, F., Oberthür, W., & Lottspeich, F. (1986) *FEBS Lett.* 205, 137–142.
- Imoto, K., Methfessel, C., Sakmann, B., Mishina, M., Mori, Y., Konno, T., Fukuda, K., Kurasaki, M., Bujo, H., Fujita, Y., & Numa, S. (1986) *Nature (London)* 324, 670–674.
- Kaldany, R. R. J., & Karlin, A. (1983) *J. Biol. Chem.* 258, 6232–6242.
- Kao, P., Dwork, A., Kaldany, R., Silver, M., Wideman, J., Stein, S., & Karlin, A. (1984) *J. Biol. Chem.* 259, 11662–11665.
- Karlin, A., Holtzman, E., Yodh, N., Lobel, P., Wall, J., & Hainfield, J. (1983) *J. Biol. Chem.* 258, 6678–6681.
- Laemmli, U. K. (1970) *Nature (London)* 227, 680–685.
- Lederer, F., Ghir, R., Guiard, B., Cortial, S., & Ito, A. (1983) *Eur. J. Biochem.* 132, 95–102.
- Mishina, M., Tobimatsu, T., Imoto, K., Tanaka, K., Fujita, Y., Fukuda, K., Kurasaki, M., Takahashi, H., Morimoto, Y., Hirose, T., Inayama, S., Takahashi, T., Kuno, M., & Numa, S. (1985) *Nature (London)* 313, 364–369.
- Muhn, P., & Hucho, F. (1983) *Biochemistry* 22, 421–425.
- Neher, E., & Steinbach, J. H. (1978) *J. Physiol. (London)* 277, 153–176.
- Neubig, R. R., Krodell, E. K., Boyd, N. D., & Cohen, J. B. (1979) *Proc. Natl. Acad. Sci. U.S.A.* 76, 690–694.



- Noda, M., Takahashi, H., Tanabe, T., Toyosato, M., Kikyo-tani, S., Hirose, T., Asai, M., Takashima, H., Inayama, S., Miyata, T., & Numa, S. (1983a) *Nature (London)* 301, 251-255.
- Noda, M., Takahashi, H., Tanabe, T., Toyosato, M., Kikyo-tani, S., Furutani, Y., Hirose, T., Takashima, H., Inayama, S., Miyata, T., & Numa, S. (1983b) *Nature (London)* 302, 528-532.
- Oberthür, W., Muhn, P., Baumann, H., Lottspeich, F., Wittmann-Liebold, B., & Hucho, F. (1986) *EMBO J.* 5, 1815-1819.
- Oswald, R. E., & Changeux, J.-P. (1981a) *Biochemistry* 20, 7166-7174.
- Oswald, R., & Changeux, J.-P. (1981b) *Proc. Natl. Acad. Sci. U.S.A.* 78, 3925-3929.
- Ratnam, M., Le Nguyen, D., Rivier, J., Sargent, P. B., & Lindstrom, J. (1986) *Biochemistry* 25, 2633-2643.
- Saitoh, T., Oswald, R., Wennogle, L. P., & Changeux, J.-P. (1980) *FEBS Lett.* 116, 30-36.
- Stroud, R. M., & Finer-Moore, J. (1985) *Annu. Rev. Cell Biol.* 1, 317-351.
- Taar, G. E., & Crabb, J. W. (1983) *Anal. Biochem.* 131, 99-107.

## Functional and Structural Characterization of the Two $\beta_1$ -Adrenoceptor Forms in Turkey Erythrocytes with Molecular Masses of 50 and 40 Kilodaltons<sup>†</sup>

Fritz Boege,<sup>‡</sup> Rolf Jürss,\* Deirdre Cooney,<sup>§,||</sup> Mirko Hekman, Alan K. Keenan,<sup>§</sup> and Ernst J. M. Helmreich

Department of Physiological Chemistry, University of Würzburg Medical School,  
D-8700 Würzburg, Federal Republic of Germany

Received July 8, 1986; Revised Manuscript Received November 7, 1986

**ABSTRACT:** We have previously described a specific protease in turkey erythrocytes that converts the larger 50-kDa (P50) form of the  $\beta_1$ -adrenoceptor to a smaller 40-kDa (P40) form [Jürss, R., Hekman, M., & Helmreich, E. J. M. (1985) *Biochemistry* 24, 3349-3354]. Further functional and structural characterization studies of the two forms are reported here. When purified P50 and P40 receptors were compared with respect to their relative capabilities to couple in lipid vesicles with pure stimulatory G-proteins ( $G_s$ -proteins) prepared from turkey erythrocytes or rabbit liver, a faster and larger activation of  $G_s$ -proteins was observed in response to *l*-isoproterenol and guanosine 5'-O-(3-thiotriphosphate) (GTP $\gamma$ S) with P40 than with P50 receptor. The  $k_{on}$  values for P40 were 0.47 min<sup>-1</sup> in the case of liver  $G_s$  and 0.22 min<sup>-1</sup> in the case of erythrocyte  $G_s$ , whereas the corresponding values for P50 were 0.34 min<sup>-1</sup> and 0.12 min<sup>-1</sup>, respectively. The binding properties of P50 and P40 forms of the receptor were not different, and desensitization of turkey erythrocytes on exposure to *l*-isoproterenol did not activate the protease. We furthermore ascertained that only the larger form with a molecular mass of 50 kDa carries the N-linked carbohydrates, which are removed on proteolytic conversion to the 40-kDa form and have either a triantennary or a tetraantennary nonfucosylated complex-type structure containing terminal sialyl residues.

We have recently reported (Jürss et al., 1985) that a receptor protease which can be inhibited by glutathione, dithiothreitol, and *o*-phenanthroline (but not by EDTA)<sup>1</sup> converts the 50-kDa  $\beta$ -adrenoceptor in turkey erythrocyte membranes to a 40-kDa polypeptide that retains the specific ligand binding site. This proteolytic conversion is partly attenuated in intact erythrocytes, presumably because of inhibition of the protease by endogenous glutathione; but it should be noted that the 40-kDa form is already detectable in varying amounts in intact erythrocytes. On the basis of these findings, we have suggested that a  $\beta_1$ -adrenoceptor-specific converting protease in the plasma membrane of turkey erythrocytes is responsible

for the conversion of the P50 to the P40 receptor. The fact that both receptor forms are present in native erythrocytes supports the assumption that the receptor conversion observed in membranes is not due to a nonspecific proteolytic artifact associated with cell lysis.

The larger 50-kDa peptide contains N-linked carbohydrates and is retained by wheat germ agglutinin-Sepharose, whereas

<sup>†</sup> This research was partly supported by SFB 176, the Fritz Thyssen Foundation, Köln, and the Fonds der Chemischen Industrie e. V. Dedicated to Professor Luis Leloir at the occasion of his 80th birthday.

\* Correspondence should be addressed to this author.

<sup>‡</sup> Part of this work has been submitted by F.B. to the Medical Faculty of the University of Würzburg in partial fulfillment of the requirements for an M.D. degree.

<sup>§</sup> Permanent address: Department of Pharmacology, University College, Dublin, Ireland.

<sup>||</sup> Recipient of a Boehringer-Ingelheim fellowship.

<sup>1</sup> Abbreviations:  $\alpha$ MeGlc, methyl  $\alpha$ -glucoside;  $\alpha$ MeMan, methyl  $\alpha$ -mannoside; BSA, bovine serum albumin; CGP 12177, Ciba Geigy Product 12177; Con A, concanavalin A; [<sup>125</sup>I]-CYP, [<sup>125</sup>I]-labeled cyano-pindolol; [<sup>125</sup>I]-CYP-Azide II, 1-(4-azidobenzoyl)-3,3-dimethyl-6-hydroxy-7-[(2-cyano-3-[[<sup>125</sup>I]iodoindol-4-yl)oxy]-1,4-diazahexane; DTT, dithiothreitol; EDTA, ethylenediaminetetraacetic acid; EGTA, ethylene glycol bis( $\beta$ -aminoethyl ether)-N,N,N',N'-tetraacetic acid; Endo F, endoglycosidase F; Endo H, endoglycosidase H; GlcNAc, N-acetyl-D-glucosamine;  $G_s$ , stimulatory G-protein; GTP $\gamma$ S, guanosine 5'-O-(3-thiotriphosphate); MOPS, 4-morpholinepropanesulfonic acid; NANA, N-acetylneuraminic acid; OMeGlcNAc, O-methyl-N-acetyl-D-glucosamine; P40 and P50, 40- and 50-kilodalton proteins of  $\beta_1$ -adrenoceptor in turkey erythrocyte membranes; PBS, phosphate-buffered saline; PMSF, phenylmethanesulfonyl fluoride; SDS, sodium dodecyl sulfate; SDS-PAGE, SDS-polyacrylamide gel electrophoresis; Tris-HCl, tris-(hydroxymethyl)aminomethane hydrochloride; WGA, wheat germ agglutinin.